SSRG International Journal of Electronics and Communication Engineering
ISSN: 2348-8549/ https://doi.org/10.14445/23488549/IJECE-V10I9P101

Volume 10 Issue 9, 1-9, September 2023

Original Article

Modified Firefly Model-Based Vector Quantization for Clinical Medical Image Compression

Preethi[1], Clara Shanthi[2], G. Kadiravan[3], Rajkumar N[4], Viji C[5], Prabhu Shankar B[6]

[1]*School of Computer Science and Information Technology, JAIN (Deemed to be University), Bangalore, Karnataka, India.*
[2]*Department of Computer Science, Mount Carmel College, Bangalore, India.*
[3]*Department of Computer Science and Engineering, Koneru Lakshmaiah Education Foundation, Vaddeswaram, AP, India.*
[4,5,6]*Department of Computer Science and Engineering, Alliance College of Engineering and Design, Alliance University, Bangalore, Karnataka, India.*

[1]*Corresponding Author : preethi.d@jainuniversity.ac.in*

Received: 03 July 2023 Revised: 15 August 2023 Accepted: 04 September 2023 Published: 30 September 2023

Abstract *- Due to the rapid increase in the usage of medical images for disease diagnosis and the rise in the volume of data produced by different medical imaging equipment, the transmission and archival of images need data compression. In the past decade, various image compression methods have been presented and find its applicability in various fields. Vector Quantization (VQ) plays a vital part in compressing images, and a Quantization Table (QT) construction is a significant process. The effectiveness of any compression technique mainly relies on the QT, generally a matrix of 64 integers. Selecting a QT is an optimization issue that bio-inspired techniques can address. The article compares two QT selection algorithms: Firefly with the Tumbling effect (FF-Tumbling) and the Teaching and Learning Based Optimization (FF-TLBO) approach. An extensive study is made between these two methods and analyzed the results. The simulation outcome is interesting in that the FF-Tumbling approach can achieve optimal reconstructed image quality, and the FF-TLBO method has the efficiency to achieve optimal compression performance.*

Keywords *- Medical imaging, Quantization, Firefly, Compression, FF-TLBO.*

1. Introduction

Presently, medical images are an essential tool in medical diagnosis. Several works have identified the connection between using medical image investigations, minimising the mortality rate, decreasing surgery requirements and maximum life expectation [1]. Consequently, the usage of medical images has rapidly increased in the past years. During the year 2003, the number of hospital visits by people in the US (age ≥ 65 years) used almost 13% of medical images [2]. Since previous medical images are stored on radiological films, the present generation digitally stores the medical images along with the maximized usage; the advancement in medical image technology outputs considerable growth in medical image numbers in the last ten years [3-5]. For instance, in 1990, a conventional Computed Tomography (CT) image of a thorax contained a set of 25 slices with 10 mm thickness, resulting in an image size of nearly 12 megabytes. In present days, the same investigation using an advanced CT machine produces a sub-mm slice thickness with high resolution [6], leading to the size of 600 megabytes to gigabytes of data [7]. In advanced hospitals, Picture Archiving and Communication Systems (PACS) manage the massive dataset's temporary and long-term archival, access, communication and computation.

Data compression is an efficient solution to solve the massive storage and distribution of data. In the earlier days of PACS, medical image compression was utilized, and efficient processes were presented earlier to famous compression standards [8]. However, some compression models significantly enhance the cost and computation needed in various systems, and the interoperable and compatible nature of these methods requires digital communication standards [9].

Image compression techniques mainly transmit images with a minimum bit count. Recognizing the data duplication in the images, ideal and appropriate encoding approaches are fundamental to any image compression technique.

Quantization can be segmented as scalar and vector quantization. VQ occurs in three stages: creating a codebook, vector encoding, and decoding [10]. The production of a codebook is an essential procedure which provides decisions related to the results of the VQ technique. The intention of generating a codebook is to identify the code vectors in a codebook for a provided collection of training vectors to minimize the average pairing-wise distance among the training vectors and their respective codewords. The vector encode functions of the VQ model involve the image's separation into multiple input blocks (or vectors) and undergo a comparison of the codewords in a codebook to find the nearest codeword for every input block. The VQ generally performs the encoding process of every input block to the codebook index. Generally, the codebook size is much smaller than the original image dataset, so the aim of compressing images is attained.

The encoded codebook will recover the interlinked sub-images at the decoding stage. Upon the reconstruction of the sub-images, the decoding process takes place [11]. Several studies have carried out the codebook design of VQ models. [12] performed the classification of VQ techniques: (1) competitive learning (2) K-Means based model. In the first model, the codebook is attained through mutual competition. The conventional first model-based group comprise self-organizing maps, neural and so on.

In recent years, bio-inspired models have been presented to construct the codebook to enhance the performance of the LGB model. [13] employed the Ant Colony System (ACS) technique for developing the codebook. Creating a codebook using ACS is done by representing coefficient vectors in a bi-directional graph.

The article compares two QT selection algorithms: Firefly with the Tumbling effect (FF-Tumbling) and the Teaching and Learning Based Optimization (FF-TLBO) approach. An extensive study is made between these two methods and analyzed the results. The simulation outcome is interesting in that the FF-Tumbling approach can achieve optimal reconstructed image quality, and the FF-TLBO method has the efficiency to achieve optimal compression performance.

2. FF-TLBO and FF-Tumbling Models

The entire process of the FF-TLBO and FF-Tumbling models are depicted in Figure 1. At the beginning stage, the image given as input undergoes partitioning into 8×8 sub-blocks. The image blocks will be quantized where the FF-Tumbling and FF-TLBO approaches determine the transform co-efficient, in which these are nearer to the topmost left corner containing the utmost crucial data.

The determined co-efficient again undergoes quantization utilizing a QT. Subsequently, the encoding procedure is carried out by the Huffman coding technique. The FF-TLBO approach determines the optimum Fitness Value (FV) for each distinct DCT block. It computes the optimum FV of the DCT block and is called the local best, where the best FV of the whole imagery is treated as the global best. The fitness function indicated in Equation (1) allocates an FV, which transforms the coefficient array.

$$f(a) = (a_1, a_2, \dots a_d)^T \quad (1)$$

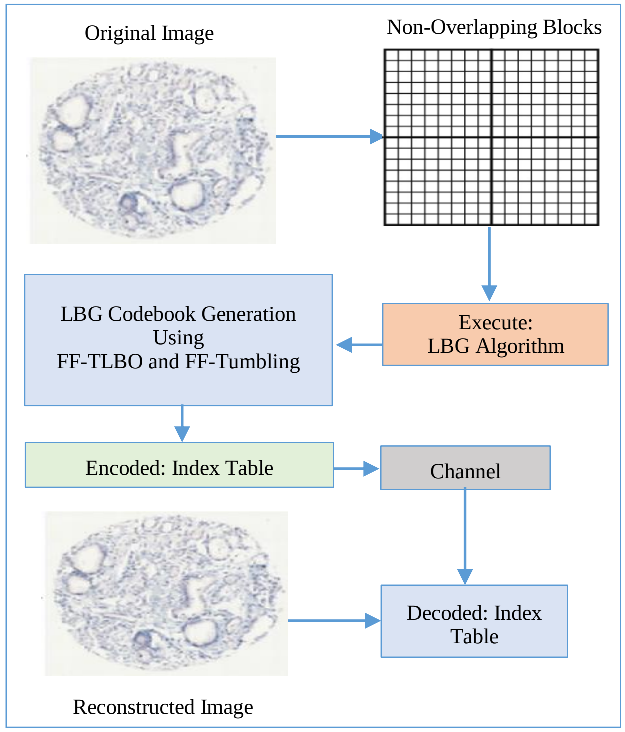

Fig. 1 Overall working principle

- Initialization: This step undergoes the initialization process where the initial population a_i, the intensity of light I_i at x_i and γ are assigned to initial values.
- Select the present optimal solution: It performs the process of choosing the optimal solution from every solution and is represented as x_i^{max},

$$a_i^{max} = arg\max_i f(a_i) \quad (2)$$

- Attractiveness: The motion of an FF a_i undergoes attraction to another FF a_j. Each solution a_j determines the FVs based on the FF's brightness.
- Stopping rule: upon exceeding the iteration number, the FF model gets terminated and offers an optimal solution.

In the case of (i) one and (ii) no brighter FF present in the search space: the FF model exhibits good results in the first case, and the FFs begin to move arbitrarily in the second case, a significant limitation of the FF algorithm. To resolve this issue, the tumbling effect and TLBO mechanisms are included in the work to derive an FF-Tumbling, and FF-TLBO approaches to discover the searching space effectively.

The TLBO method originated from sharing knowledgebase among teachers and students during the learning process. It is also based on the teacher's impact on the class performance. Two levels exist in the TLBO model: 'Teacher level' and 'Training level'. The behaviour of the efficient teacher tries to enhance the understanding level to the greatest extent. However, practically, it is tedious, and the teacher could achieve the average class to a particular stage depending upon diverse aspects.

For example, M_i and T_i represents the class average value and teacher in any iteration i. The T_i tries to go towards the mean M_i nearer to their level, so the fresh mean will be T_i called M_{new}. The solution is upgraded based on the current and fresh mean variation. M_{new} as equated below.

$$Difference\_Mean_i = r_i(M_{new} - T_F M_i) \tag{3}$$

Where, T_F depicts the teaching aspect that plays a determining factor for the value of mean to be altered and r_i depicts a randomized number present inside [0, 1]. The value of T_F can be 1 or 2 that are selected randomly, as

$$TF = round\,[1 + rand\,(0,1)\{2 - 1\}] \tag{4}$$

This variation will modify the available solution as given as follows.

$$X_{new,\ i} = X_{old,\ i} + Difference\_Mean_i \tag{5}$$

Learners will improve their knowledge by utilising two ways: first, they receive the teacher's input and then interact with one another. A learner could enhance their knowledge by interacting randomly with other learners. Generally, the learner's knowledge interacts with a more knowledgeable learner. In such cases, the learner alteration is applied as follows.

For $\mathrm{i} = 1 : \mathrm{P_n}$

Arbitrary choose two learners $\mathrm{A_i}$ and $\mathrm{A_j}$, where $\mathrm{i} \neq \mathrm{j}$

If $\mathrm{f(A_i) < f(A_j)}$

$$\mathrm{A_{n,i} = A_{o,i} + r_i(A_i - A_j)}$$

Else

$$\mathrm{A_{n,i} = A_{o,i} + r_i(A_j - A_i)}$$

End If

End For

Allow X_n When an enhanced function value is attained. Upon the reception of the compressed images, the reconstruction process reversibly occurs. The input image undergoes portioning to the 8*8 blocks of sub-images, and then the tumbling effect determines the optimal FV of every DCT block. In this technique, the fitness function value chooses the movement of FFs. When the FF shifts towards the fitness function, it is called swimming. Otherwise, the movement of FF takes place through the motion of bacteria. The motion of FFs follows the chemotactic motion of bacterium and is defined as follows:

$$= a_i^{t-1} + v_i^t \frac{\Delta_i}{\sqrt{\Delta_i^T \times \Delta_i}} \tag{6}$$

3. Performance Evaluation

An experimental evaluation occurs in the benchmark medical imagery to analyze the outputs attained by the FF-Tumbling and FF-TLBO approaches, as shown in Figure 2 [14]. The type of medical images applied for validation is diatom, diabetic retinopathy, and mammographic images. The reconstructed image's visual quality ensures an efficient output on the compression performance. Figure 3 and Figure 4 illustrate the sample reconstructed images attained by FF-TLBO and FF-Tumbling models, respectively. These figures show that the reconstructed image looks clear by the presented FF-TLBO model compared to the FF-Tumbling method.

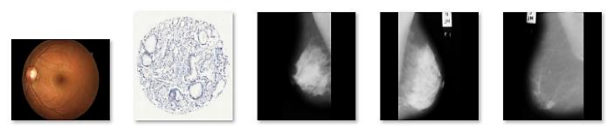

Fig. 2 Sample test images

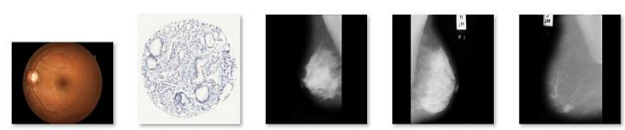

Fig. 3 Reconstructed images using proposed FF-TLBO

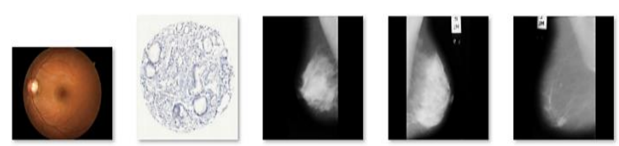

Fig. 4 Reconstructed images using proposed FF-tumbling

Figures 5-7 show the analysis of compression performance among three models regarding CR, SS and Bit Rate (BR) subsequently. Table 1 compares the DCT with the FF-TLBO and FF-Tumbling approaches concerning BR, CR, and SS on the set of 5 test images.

On the applied image '13_left', the FF-TLBO approach shows maximum compression performance with a CR of 0.02770, SS of 97.2301 and BR of 0.6650. Simultaneously, the FF-Tumbling technique offers slightly lesser compression performance with a CR of 0.09875, SS of 90.1249 and BR of 2.3710. However, the existing DCT model shows poor compression performance with a maximum CR of 0.10514, a BR of 2.5242 and a minimum SS of 89.4864, respectively. Among the three compared methods, the FF-TLBO method is more efficient than the other methods. The lower values of CR and BR imply that the FF-TLBO approach attained optimal compression performance.

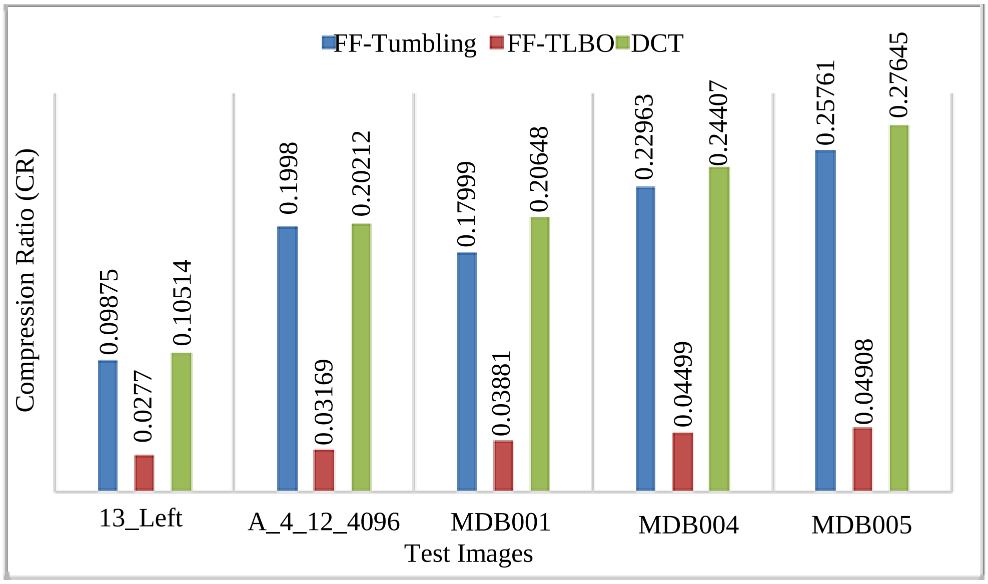

Fig. 5 Compression performance analysis among three models of CR

Table 1. Comparison of DCT with the proposed models about compression effectiveness

Images (Name)	Compression Ratio (CR)			Space Savings			BR		
	FF-Tumbling	FF-TLBO	DCT	FF-Tumbling	FF-TLBO	DCT	FF-Tumbling	FF-TLBO	DCT
13_left	0.09875	0.02770	0.10514	90.1249	97.2301	89.4864	2.3710	0.6650	2.5242
A_4_12_4096	0.19980	0.03169	0.20212	80.0204	96.8315	79.7882	4.7951	0.7605	4.8508
mdb001	0.17999	0.03881	0.20648	82.0013	96.1191	79.3523	1.4414	0.3108	1.6535
mdb004	0.22963	0.04499	0.24407	77.0368	95.5010	75.5927	1.8389	0.3603	1.9546
mdb005	0.25761	0.04908	0.27645	74.2391	95.0925	72.3545	2.0630	0.3930	2.2139

Table 2. Comparison of DCT with proposed models about compressed size and packet size

Images (Name)	Original Size (Bytes)	Compression Size			Original Packet Size (Bytes)	Packet Size		
		FF-Tumbling	FF-TLBO	DCT		FF-Tumbling	FF-TLBO	DCT
13_left	15116598	1492784	418718	1492784	521262.00	51475.31	418718	54803.34
A_4_12_4096	50331702	10056055	1594781	10172943	1735575.93	346760.52	54992.45	350791.14
mdb001	1049654	188924	40736	216729	36194.97	6514.62	1404.69	7473.41
mdb004	1049654	241034	47224	256192	36194.97	8311.52	1628.41	8834.21
mdb005	1049654	270400	51512	290182	36194.97	9324.14	1776.28	10006.28

On the applied image 'A_4_12_4096', the FF-TLBO approach shows maximum compression performance with a CR of 0.03169, SS of 96.8315 and BR of 0.7605. Simultaneously, the FF-Tumbling technique offers slightly lesser compression performance with a CR of 0.19980, SS of 80.0204 and BR of 4.7951. However, the existing DCT model shows poor compression performance with a maximum CR of 0.10514, a BR of 4.8508 and a minimum SS of 79.7882, respectively. On the applied image 'mdb001', the FF-TLBO approach shows maximum compression performance with a CR of 0.03881, SS of 96.1191 and BR of 0.3108. Simultaneously, the FF-Tumbling technique offers slightly lesser compression performance with a CR of 0.17999, SS of 82.0013, and BR of 1.4414. However, the existing DCT model shows poor compression performance with a maximum CR of 0.20648, a BR of 1.6535 and a minimum SS of 79.3523, respectively. On the applied image 'mdb004', the FF-TLBO approach shows maximum compression performance with the CR of 0.04499, SS of 95.5010and BR of 0.3603. Simultaneously, the FF-Tumbling method offers slightly lesser compression performance with a CR of 0.22963, SS of 77.0368 and BR of 1.8389.

However, the existing DCT model shows poor compression performance with a maximum CR of 0.24407, a BR of 1.9546 and a minimum SS of 75.5927, respectively. On the applied image ' mdb005', the FF-TLBO approach shows maximum compression performance with a CR of 0.04908, SS of 95.0925 and BR of 0.3930. Simultaneously, the FF-Tumbling method offers slightly lesser compression performance with the CR of 0.25761, SS of 74.2391and BR of 2.0630. However, the existing DCT model shows poor compression performance with a maximum CR of 0.27645, a BR of 2.2139and a minimum SS of 72.3545, respectively.

Another aspect of results validation occurs concerning the compression and packet size to verify the better compression performance among the three methods. The attained outputs are tabulated in Table 2 and Figures 8 and 9. From Table 2, on the applied test image '13_left', it is clear that the FF-TLBO technique requires minimum compression and packet sizes of 418718 and 418718, respectively. In addition, on the same image, the FF-Tumbling method requires a slightly higher compression size and packet size of 1492784 and 51475.31, respectively.

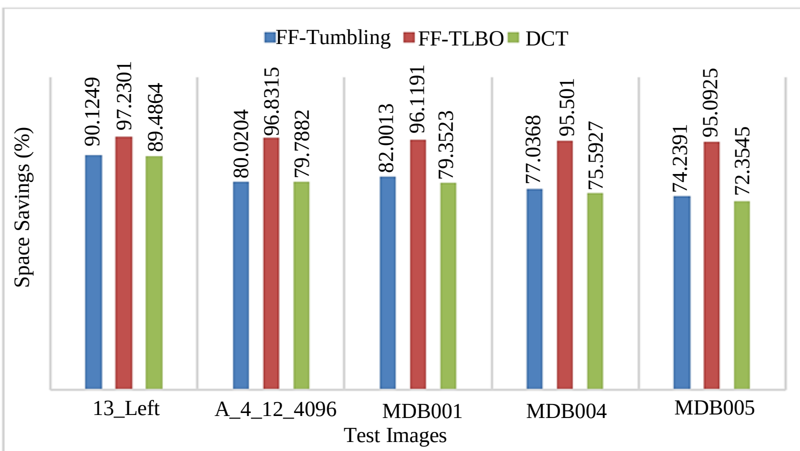

Fig. 6 Compression performance analysis among three models with regard to SS

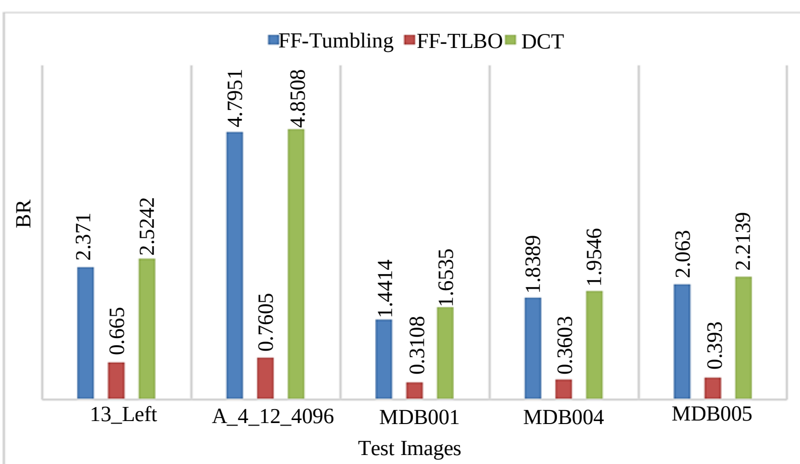

Fig. 7 Compression performance analysis among three models with regard to BR

In the same way, the DCT method effectively compresses the applied images by attaining lower compression size and packet size of 1492784 and 54803.34, respectively. The applied test image ‘A_4_12_4096’ shows the FF-TLBO technique requires minimum compression and packet sizes of 1594781 and 54992.45, respectively. In addition, on the same image, the FF-Tumbling method requires a slightly higher compression size and packet size of 10056055 and 346760.52, respectively. In the same way, the DCT method effectively compresses the applied images by attaining lower compression size and packet size of 10172943 and 350791.14, respectively. Similarly, on the employed test image ‘mdb001’, it is evident that the FF-TLBO technique needs minimum compression and packet sizes of 40736 and 1404.69, respectively. In addition, on the same image, the FF-Tumbling method requires slightly higher compression size and packet size of 188924 and 6514.62, respectively. In the same way, the DCT method effectively compresses the applied images by attaining lower compression size and packet size of 216729 and 8834.21, respectively.

Similarly, on the applied test image ‘mdb004’, it is evident that the FF-TLBO technique requires minimum compression size and packet size of 47224 and 1628.41, respectively. In addition, on the same image, the FF-Tumbling method requires a slightly higher compression size and packet size of 241034 and 8311.52 respectively. In the same way, the DCT method shows ineffectiveness in compressing the applied images by attaining lower compression size and packet size of 256192 and 8834.21 subsequently.

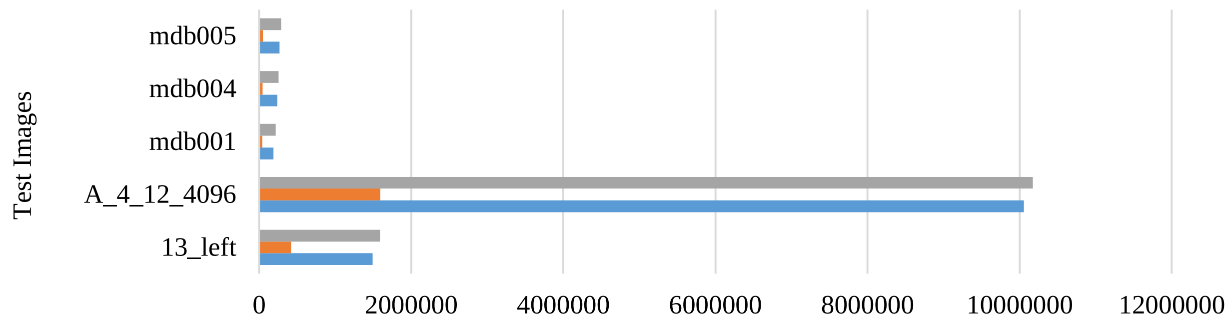

	13_left	A_4_12_4096	mdb001	mdb004	mdb005
DCT	1589297	10172943	216729	256192	290182
FF-TLBO	418718	1594781	40736	47224	51512
FF-Tumbling	1492784	10056055	188924	241034	270400

Compressed File Size (Bytes)

Fig. 8 Compression performance analysis among three models concerning compressed file size

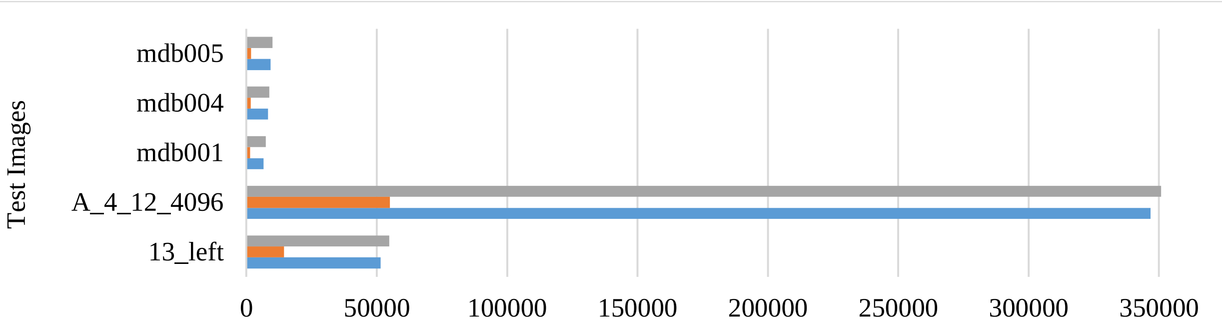

	13_left	A_4_12_4096	mdb001	mdb004	mdb005
DCT	54803.34	350791.14	7473.41	8834.21	10006.28
FF-TLBO	14438.55	54992.45	1404.69	1628.41	1776.28
FF-Tumbling	51475.31	346760.52	6514.62	8311.52	9324.14

Compressed Packet Size (Bytes)

Fig. 9 Compression performance analysis among three models concerning compressed packet size

At last, on the applied test image 'mdb005', it is evident that the FF-TLBO technique requires minimum compression and packet sizes of 51512 and 1776.28, respectively. In addition, on the same image, the FF-Tumbling method requires slightly higher compression size and packet size of 270400 and 9324.14, respectively.In the same way, the DCT method effectively compresses the applied images by attaining lower compression size and packet size of 290182 and 10006.28 subsequently.To validate the effectiveness of the FF-TLBO and FF-Tumbling approaches on medical images, assessing these methods concerning reconstructed image quality becomes mandatory. Here, a reconstructed image quality analysis concerning MSE, SNR and PSNR is made. Table 3 and Figures 10-12 compares results obtained by three methods concerning MSE, SNR and PSNR.

On the applied 13_left image, the FF-Tumbling method shows Better Reconstructed Image Quality (BRIQ) with a minimum MSE of 1.039, maximum SNR and PSNR of 42.598 and 57.504, respectively.

On the other hand, the FF-TLBO method shows slightly Poor Reconstructed Image Quality (PRIQ) with the MSE, SNR and PSNR values of 10.176, 32.691 and 47.597, respectively. However, the DCT shows PRIQ with the highest MSE of 15.892, lowest SNR and PSNR of 30.5671 and 45.661, respectively.

On the applied A_4_12_4096 image, the FF-Tumbling method shows BRIQ with a minimum MSE of 1.436, maximum SNR and PSNR of 50.376 and 56.101, respectively. On the other hand, the FF-TLBO method shows slightly PRIQ with the MSE, SNR and PSNR values of 14.249, 40.412 and 56.101, respectively. However, the DCT shows PRIQ with the highest MSE of 20.357, lowest SNR and PSNR of 38.8923 and 44.586, respectively.

Table 3. Comparison of DCT with proposed models concerning image quality

Images (Name)	MSE			SNR			PSNR		
	FF-Tumbling	FF-TLBO	DCT	FF-Tumbling	FF-TLBO	DCT	FF-Tumbling	FF-TLBO	DCT
13_left	1.039	10.176	15.892	42.598	32.691	30.5671	57.504	47.597	45.661
A_4_12_4096	1.436	14.249	20.357	50.376	40.412	38.8923	56.101	46.135	44.586
mdb001	0.115	2.294	3.892	51.434	38.451	36.2901	67.047	54.067	51.772
mdb004	0.154	3.033	4.390	53.046	40.113	37.2161	65.787	52.855	51.249
mdb005	0.162	3.677	4.289	52.229	38.672	37.1290	65.575	52.018	51.350

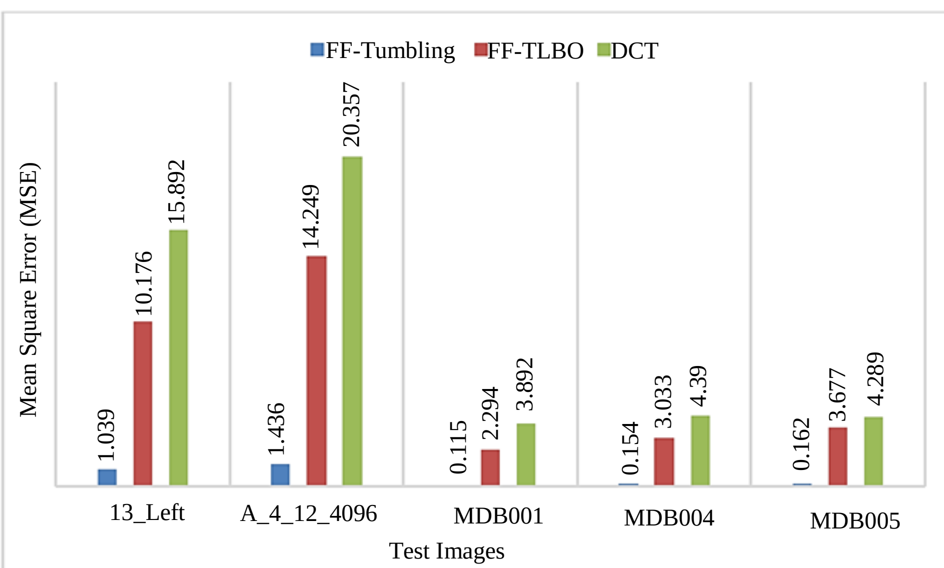

Fig. 10 Reconstructed image quality evaluation concerning MSE

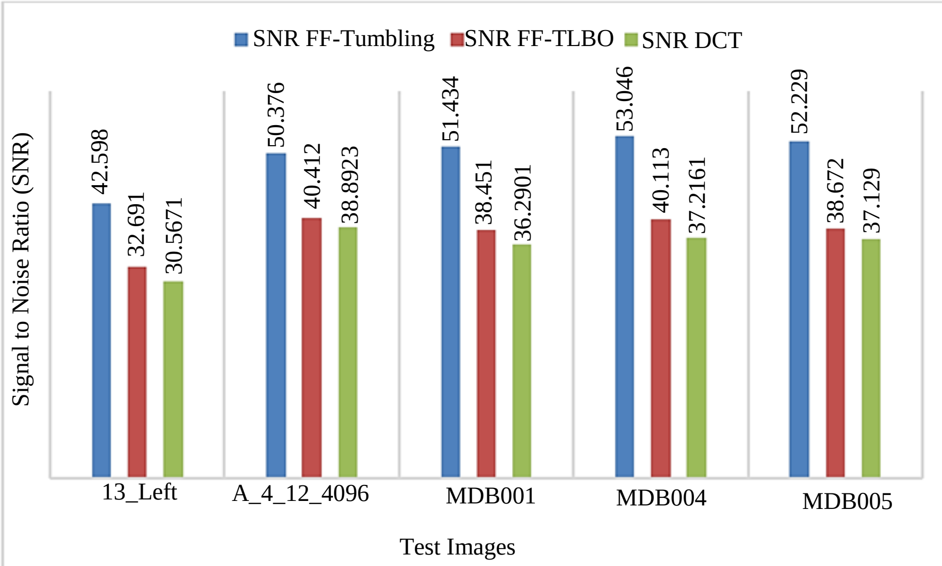

Fig. 11 Reconstructed image quality evaluation concerning SNR

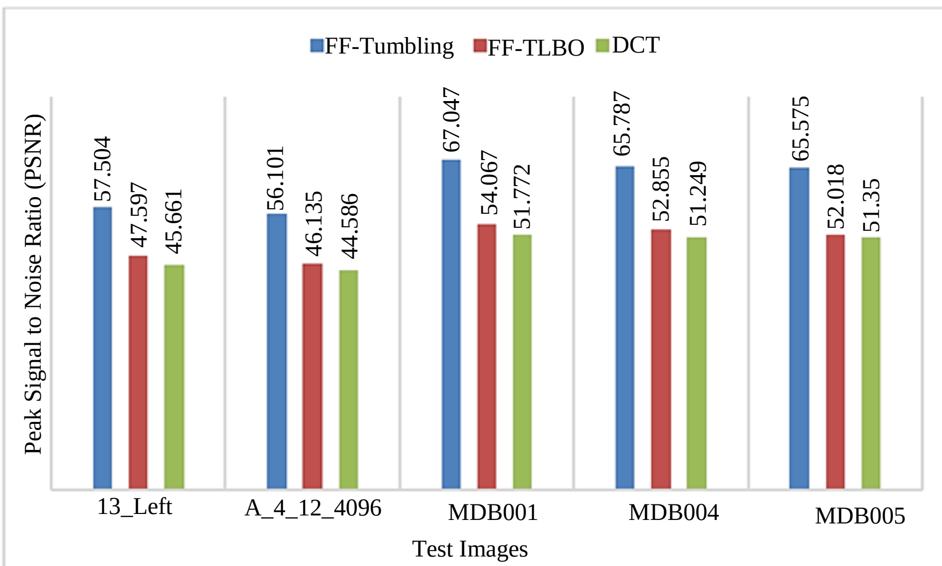

Fig. 12 Reconstructed image quality evaluation concerning PSNR

On the applied mdb001 image, the FF-Tumbling method shows BRIQ with a minimum MSE of 0.115, maximum SNR and PSNR of 51.434 and 67.047, respectively.

On the other hand, the FF-TLBO method shows slight PRIQ with the MSE, SNR and PSNR values of 2.294, 38.451 and 54.067, respectively. However, the DCT shows PRIQ with the highest MSE of 3.892, lowest SNR and PSNR of 36.2901 and 51.772, respectively.

On the applied mdb004 image, the FF-Tumbling method shows BRIQ with a minimum MSE of 0.154, maximum SNR of 53.046 and maximum PSNR of 65.787, respectively. On the other hand, the FF-TLBO method shows slight PRIQ with the MSE, SNR and PSNR values of 3.033, 40.113 and 52.855, respectively. However, the DCT shows PRIQ with the highest MSE of 4.390, lowest SNR and PSNR of 37.2161 and 51.249, respectively.

On the applied mdb005 image, the FF-Tumbling method shows BRIQ with a minimum MSE of 0.162, maximum SNR and PSNR of 52.229 and 65.575, respectively. On the other hand, the FF-TLBO method shows slightly PRIQ with the MSE, SNR and PSNR values of 3.677, 38.672 and 52.018, respectively. However, the DCT shows PRIQ with the highest MSE of 4.289, lowest SNR and PSNR of 37.1290 and 51.350, respectively.

4. Conclusion

In recent years, bio-inspired models have been presented to construct the codebook to improve the achievement of the LGB approach. In the present article, a comparative evaluation of two QT selection approaches occurs Firefly with Tumbling effect (FF-Tumbling) and Firefly with Teaching and Learning Based Optimization (FF-TLBO) approaches. An extensive study is made between these two methods and analyzed the results.

The simulation outcome is interesting in that the FF-Tumbling method can achieve optimal reconstructed image quality, and the FF-TLBO method has the efficiency to achieve optimal compression performance.

References

[1] R. Duszak, and L. Harvey, "Medical Imaging: Is the Growth Boom over? The Neiman Report," *Neiman Health Policy Institute*, 2012. [Google Scholar] [Publisher Link]

[2] Martey S. Dodoo, Richard Duszak, and Danny R. Hughes, "Trends in the Utilization of Medical Imaging from 2003 to 2011: Clinical Encounters Offer a Complementary Patient-Centered Focus," *Journal of the American College of Radiology*, vol. 10, no. 7, pp. 507-512, 2013. [CrossRef] [Google Scholar] [Publisher Link]

[3] Vaishali Patel, and Anand Mankodia, "Deep Learning in Medical Image Super-Resolution: A Survey," *International Journal of Engineering Trends and Technology*, vol. 71, no. 8, pp. 1-12, 2023. [CrossRef] [Publisher Link]

[4] P. Kanmani, P. Marikkannu, and M. Brindha, "A Medical Image Classification Using ID3 Classifier," *SSRG International Journal of Computer Science and Engineering*, vol. 3, no. 10, pp. 8-11, 2016. [CrossRef] [Publisher Link]

[5] M. Amirthalingam, and R. Ponnusamy, "Automated Wireless Capsule Endoscopy Image Classification Using Reptile Search Optimization with Deep Learning Model," *International Journal of Engineering Trends and Technology*, vol. 71, no. 4, pp. 274-283, 2023. [CrossRef] [Publisher Link]

[6] Janani S., and D.F.X. Christopher, "Conditional Super Resolution Generative Adversarial Network for Cervical Cell Image Enhancement," *SSRG International Journal of Electrical and Electronics Engineering*, vol. 10, no. 4, pp. 70-76, 2023. [CrossRef] [Publisher Link]

[7] V. Baby Deepa, and R. Malathi, "A Review of Image Processing in Different Techniques," *International Journal of Computer and Organization Trends*, vol. 10, no. 5, pp. 12-15, 2020. [CrossRef] [Publisher Link]

[8] I.W. Van Aken et al., "Compressed Medical Images and Enhanced Fault Detection within an ARC-NEMA Compatidle Picture Archiving and Communications System," *Medical Imaging*, vol. 767, 1987. [CrossRef] [Google Scholar] [Publisher Link]

[9] David A. Clunie, "What is Different about Medical Image Compression," *IEEE Communication Society-Multimedia Communications Technical Committee E-Letter*, vol. 6, no. 7, pp. 31-37, 2011. [Google Scholar]

[10] Chin-Chen Chang, Yu-Chiang Li, and Jun-Bin Yeh, "Fast Codebook Search Algorithms Based on Tree-Structured Vector Quantization," *Pattern Recognition Letters*, vol. 27, no. 10, pp. 1077-1086, 2006. [CrossRef] [Google Scholar] [Publisher Link]

[11] Yogesh Kumar Sharma, Amit Mishra, and Amit Sharma, "An Advanced Approach for Image Steganography Method," *International Journal of Computer and Organization Trends*, vol. 9, no. 4, pp. 1-4, 2019. [CrossRef] [Publisher Link]

[12] Giuseppe Patané, and Marco Russo, "The Enhanced LBG Algorithm," *Neural Networks*, vol. 14, no. 9, pp. 1219-1237, 2001. [CrossRef] [Google Scholar] [Publisher Link]

[13] Nasir Rajpoot et al., "A Novel Image Coding Algorithm Using Ant Colony System Vector Quantization," *International Workshop on Systems, Signal and Image Processing*, Poland, 2004. [Google Scholar] [Publisher Link]

[14] Kaggle, Diabetic Retinopathy Detection, Dataset Description, 2015. [Online]. Available: https://www.kaggle.com/c/diabetic-retinopathy-detection/data